

Received March 12, 2021, accepted April 28, 2021, date of publication May 17, 2021, date of current version June 2, 2021.

Digital Object Identifier 10.1109/ACCESS.2021.3080705

Characterizing Human Postural Stability by Using Features Extracted From the Correlation Structure of Ground Reaction Force Components

JIA-LI SUNG¹, LAN-YUEN GUO², CHIN-HSUAN LIU^{3,4}, POSEN LEE⁴, CHEN-WEN YEN^{1,5,6}, AND LIH-JIUN LIAW^{5,6,7,8}

¹Department of Mechanical and Electro-Mechanical Engineering, National Sun Yat-sen University, Kaohsiung 80424, Taiwan

²Department of Sports Medicine, Kaohsiung Medical University, Kaohsiung 80708, Taiwan

³Department of Occupational Therapy, Kaohsiung Municipal Kai-Syuan Psychiatric Hospital, Kaohsiung 80276, Taiwan

⁴Department of Occupational Therapy, I-Shou University, Kaohsiung 82445, Taiwan

⁵Department of Physical Therapy, College of Health Science, Kaohsiung Medical University, Kaohsiung 80708, Taiwan

⁶Neuroscience Research Center, Kaohsiung Medical University, Kaohsiung 80708, Taiwan

⁷Department of Physical Medicine and Rehabilitation, Kaohsiung Medical University Chung-Ho Memorial Hospital, Kaohsiung 80708, Taiwan

⁸Department of Medical Research, Kaohsiung Medical University Hospital, Kaohsiung 80708, Taiwan

Corresponding authors: Chen-Wen Yen (vincen@mail.nsysu.edu.tw) and Lih-Jiun Liaw (lijili@kmu.edu.tw)

This work was supported in part by the Ministry of Science and Technology in Taiwan under Grant 106-2221-E-110-044 and Grant MOST 107-2221-E-110-073.

This work involved human subjects or animals in its research. Approval of all ethical and experimental procedures and protocols was granted by Kaohsiung Medical University under Application No. KMUHIRB-E(I)-20180072.

ABSTRACT A force plate is one of the most popular tools for postural stability assessment. It decomposes the ground reaction force (GRF) applied to the human body into multiple force components to determine the center of pressure (COP), which is the point at which the GRF is applied. Many COP measures have been proposed to characterize postural stability. Despite postural stability being closely related to GRF components, the interactions between them have rarely been studied. By studying the correlation structure of these GRF components, we developed a set of features to assess postural stability. We determined the correlation matrix of these GRF components and subsequently solved the corresponding eigenvalue problem; we used the resulting eigenvalues to characterize postural stability. The effectiveness of the proposed features was demonstrated by using them to differentiate between individuals in two age groups: 18–24 and 65–73 years. Statistical test results showed that the correlation matrix eigenvalues of the two age groups differed significantly. The classification results demonstrated that most of the correlation matrix eigenvalues were more sensitive to age variations than one of the most reliable and accurate conventional COP features. Furthermore, by reducing the force sensing requirement from three-dimensional to one-dimensional by considering only the vertical GRF components, a simplified version of the proposed approach can be obtained, which could reduce the cost of the force plate system substantially.


INDEX TERMS Correlation structure, force plates, ground reaction force, postural control, quiet standing.

I. INTRODUCTION

The center of pressure (COP) is defined as the point at which the ground reaction force (GRF) is applied to the human body. Our postural control system must adaptively adjust the position of the COP to generate stabilizing moments to maintain postural balance [1], [2]. By decomposing the

GRF into multiple force components, force plates can easily determine the location of the COP. For the remainder of the manuscript, the GRF components that have been obtained by the force plates will be referred to as FP-GRF signals.

Owing to the critical role of the COP in postural balance and the ease with which force plates can be used, COP features have been employed in approximately 60% of the published literature on postural control [3], [4]. Many COP features have been proposed for assessing the

The associate editor coordinating the review of this manuscript and approving it for publication was Venkata Rajesh Pamula .

impacts of different health-related conditions on postural stability; these health-related conditions include aging [5], [6], peripheral neuropathy [7], musculoskeletal disorders [8], stroke [9], [10], spinal cord injury [11], concussion [12], cancer [13], frailty syndrome [14], symptomatic degenerative lumbar disease [15], Parkinson's disease [16], [17], multiple sclerosis [18], [19], and fall risk [20]. In addition, COP features have also been used to assess the impacts of special events such as pregnancy. However, despite the widespread use of the COP in assessing postural stability, the FP-GRF signals associated with the COP have rarely been studied [21].

Based on random matrix theory (RMT) developed by Wigner *et al.* [22]–[26], the correlation structure method represents a systematic approach for studying multivariate time series. By characterizing the interactions between multiple channels of signals with the eigenvalues and eigenvectors of the correlation matrix, the correlation structure method has been used to analyze the multivariate time series associated with financial data [27], [28], magnetoencephalography recordings [29], climate data [30], internet traffic [31], and electroencephalograms [32]–[35]. However, to the best of our knowledge, the correlation structure of the FP-GRF signals has never been studied. Therefore, in this work, we introduce a set of features to assess postural stability by extracting features from the correlation structure of the FP-GRF signals (hereafter, the GRF correlation structure). The effectiveness of the proposed features was verified by using them to differentiate between individuals belonging to two age groups via experiments in which the individuals were asked to be in the quiet standing posture. The assumption is that if the proposed features can outperform the conventional measures used in detecting the effects of aging on postural stability, then the use of the proposed features as general postural stability measures would warrant further investigation.

Compared to conventional methods which assess postural stability by using features extracted from two-dimensional COP motion, a novelty of the proposed approach is that postural stability features are extracted from eight channels of FP-GRF signals. In addition, by using RMT to study the GRF correlation structure, this work introduces a new theoretical framework for postural stability assessment.

II. METHODS

A. EXPERIMENTAL PROCEDURE

The volunteers participating in this study belonged to two age groups—a younger age group (20.1 ± 1.29 years, range 18–24 years; BMI 22.5 ± 3.21 kg/m²) and an older age group (68.7 ± 2.96 years, range 65–73 years; BMI 23.9 ± 4.13 kg/m²). Each group consisted of ten healthy men and ten healthy women. Based on self-reports and physical examinations, we verified that no participant had a pathological condition that would compromise their postural performance. The experimental procedures were approved by the Institutional Review Board of the Kaohsiung Medical

University Chung-Ho Memorial Hospital, Kaohsiung, Taiwan. Written informed consent was obtained from participants before the test.

Every participant was tested in two experimental sessions per day for 2 days. Each session included three 80 s eyes-open–closed trials. Consequently, each test participant underwent 12 trials (3 trials/session \times 4 sessions). In the first 40 s of the trials, the participants were asked to look straight ahead at a visual reference and stand quietly (with arms at the side) in a comfortable stance near the center of the force plate. Subsequently, under the same test conditions, the participants were asked to close their eyes for the remaining 40 s of the trial. The trials and sessions were separated by approximately 1 and 5 min of rest, respectively. Unless otherwise specified, the data collected between 5 s and 35 s in the eyes-open trials were used for this study.

The measurement system consisted of a force plate (9286AA, Kistler Instrumente AG) connected to a PC-based data acquisition system. The force plate measurements were sampled at 512 Hz with a 14-bit analog-to-digital data acquisition card (USB-6009, National Instruments, Austin, TX) connected to a desktop PC. The data processing software was a custom-developed program written in LabVIEW (National Instruments, Austin, TX). The signals were filtered using a zero-phase sixth-order low-pass Butterworth filter with a 5-Hz cutoff frequency.

B. CORRELATION STRUCTURE METHOD

The first step in the correlation structure method is to determine the correlation matrix of the multivariate time series to study the interdependencies between N channels of signals. The i -th row and j -th column of the correlation matrix is specified as the Pearson product-moment correlation coefficient between the i -th and j -th signals; it is denoted as c_{ij} . The correlation matrix, denoted as \mathbf{C} , is a real N by N symmetric matrix with diagonal terms $c_{ii} = 1$. To study the correlation structure of these signals, we then solve the eigenvalue problem

$$(\mathbf{C} - \lambda_i \mathbf{I})\mathbf{v}_i = \mathbf{0} \quad (1)$$

to determine the eigenvalues λ_i and eigenvectors \mathbf{v}_i for $i = 1, \dots, N$. In (1), \mathbf{I} is an N -dimensional identity matrix and $\mathbf{0}$ is an N -dimensional vector whose elements are all zero. Through linear algebra, it can be shown that the resulting eigenvalues are always real and that the corresponding eigenvectors are orthogonal to one another. Using linear algebra, we can also show that the sum of the eigenvalues is N . That is, $\lambda_1 + \lambda_2 + \lambda_3 + \dots + \lambda_N = N$, and the value λ_i is proportional to the amount of correlation in the direction of its eigenvector \mathbf{v}_i . The eigenvalues are arranged in ascending order such that $\lambda_{min} = \lambda_1 \leq \lambda_2 \leq \lambda_3 \dots \leq \lambda_N = \lambda_{max}$; these eigenvalues are called the spectrum of the correlation matrix. Notably, this spectrum plays a central role in characterizing the correlation structure of a multivariate time series.

After solving the eigenvalue problem, most previous studies attempted to use the information provided by the

eigenvalues and eigenvectors to separate genuine correlations from random correlations. By assuming the number of signals $N \rightarrow \infty$, the number of data points of each of these signals $L \rightarrow \infty$, and $Q = L/N \geq 1$, the probability distribution function of the correlation matrix eigenvalues of independent Gaussian signals can be represented as [36]:

$$\rho(\lambda) = \frac{Q\sqrt{(\lambda_+ - \lambda)(\lambda_- - \lambda)}}{2\pi\sigma^2\lambda} \quad (2)$$

where

$$\lambda_- = \sigma^2 \left(1 + \frac{1}{Q} - 2\sqrt{\frac{1}{Q}} \right), \lambda_+ = \sigma^2 \left(1 + \frac{1}{Q} + 2\sqrt{\frac{1}{Q}} \right) \quad (3)$$

with λ_- and λ_+ representing the lower and upper bounds of the eigenvalues, respectively. Hereafter, the eigenvalues outside the RMT bounds of (3) are referred to as displaced eigenvalues.

When signals are all mutually independent and thus uncorrelated, the correlation matrix should be an identity matrix. However, because of the finite size of the time window used to construct the correlation matrix, the off-diagonal elements of the correlation matrix are generally not zero even when the signals are completely independent. Equation (3) is used to determine the lower and upper bounds of the correlation matrix eigenvalues for such random correlation results; therefore, (3) provides a guideline for identifying nonrandom correlations. The presence of displaced eigenvalues implies the existence of nonrandom correlations. Therefore, by identifying displaced eigenvalues, one can differentiate physically meaningful correlation modes from the background noise by using RMT [30], [32], [34]. A more rigorous and complete introduction to RMT is beyond the scope of this work. Interested readers are referred to papers and books such as [32] and [37]–[39].

Studying the correlation structure of a multivariate time series by using the results of RMT has several limitations. First, the requirements of $N \rightarrow \infty$ and $L \rightarrow \infty$ are difficult to meet when dealing with real-world signals. Second, the results of RMT are invalid for nonstationary time series. Third, interpreting the eigenvalue statistics is often very difficult [30], [39]. Therefore, instead of studying the GRF correlation structure analytically, we directly tested the effectiveness of the correlation matrix eigenvalues in characterizing postural stability by differentiating between individuals belonging to two age groups via the quiet standing experiments described in the previous section.

C. GRF COMPONENTS OBTAINED BY FORCE PLATE

A force plate, which is shown in Fig. 1, is a simple mechanical device. In Fig. 1, the x , y , and z axes correspond to the medial–lateral (ML), anterior–posterior (AP), and vertical directions, respectively, whereas the origin of the coordinate system is chosen as the geometrical center of the force plate. In addition, d_x and d_y represent the distances along the x and

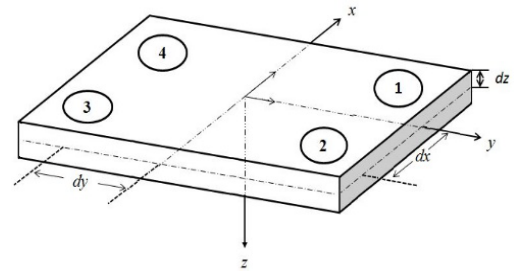


FIGURE 1. Force plate with its coordinate system and three geometrical parameters. The locations of four force sensors on the force plate are also shown.

y axes, respectively, from the coordinate axes to the force sensors, and d_z is the distance along the z axis from the origin of the coordinate system to the support surface of the force plate.

With force transducers positioned at the four corners of the force plate, F_i denoting the GRF component at the i -th corner of the force plate, and f_x, f_y , and f_z denoting the GRF components in the ML, AP, and vertical directions, respectively, the resultant GRF can be expressed as the following vector f :

$$f = f_x i + f_y j + f_z k = F_1 + F_2 + F_3 + F_4 \quad (4)$$

where i, j , and k are unit vectors along the x, y , and z axes, respectively. By denoting F_{iz} as the vertical component of F_i , the vertical component of the resultant GRF f can be written as

$$f_z = F_{1z} + F_{2z} + F_{3z} + F_{4z} \quad (5)$$

Similarly, the ML and AP components of the resultant GRF f can be represented as

$$f_x = F_{1x} + F_{2x} + F_{3x} + F_{4x} \quad (6)$$

$$f_y = F_{1y} + F_{2y} + F_{3y} + F_{4y} \quad (7)$$

where F_{ix} and F_{iy} are the ML and AP components of F_i , respectively. The force plate employed in this work uses eight FP-GRF signals to compute the COP. These FP-GRF signals are $F_{12x} = F_{1x} + F_{2x}, F_{34x} = F_{3x} + F_{4x}, F_{14y} = F_{1y} + F_{4y}, F_{23y} = F_{2y} + F_{3y}, F_{1z}, F_{2z}, F_{3z},$ and F_{4z} . Using Newtonian mechanics, we derive the following equations, which can then be used to determine the coordinates of the COP.

$$COP_x = \frac{d_x (F_{14z} - F_{23z}) + d_z (F_{12x} + F_{34x})}{F_{1z} + F_{2z} + F_{3z} + F_{4z}} \quad (8)$$

$$COP_y = \frac{d_y (F_{12z} - F_{34z}) + d_z (F_{14y} + F_{23y})}{F_{1z} + F_{2z} + F_{3z} + F_{4z}} \quad (9)$$

For a given COP position, (8) and (9) represent two balance task constraints imposed on the FP-GRF signals. Another balance task during quiet standing is control of the rotation about the center of mass of the human body in the vertical direction [40]. When standing on a force plate, the free

moment (FM) applied to the human body can be represented as [41], [42]:

$$FM = -d_x(F_{14y} - F_{23y}) + d_y(-F_{12x} + F_{34x}) - COP_x(F_{14y} + F_{23y}) + COP_y(F_{12x} + F_{34x}) \quad (10)$$

As a frictional torque, FM also needs to be appropriately controlled to prevent our body from rotating excessively in the vertical direction. Therefore, (10) represents another constraint imposed on FP-GRF signals.

With the balance task constraints of (8) - (10), it is evident that the FP-GRF signals cannot be all mutually independent. Consequently, we hypothesize that the GRF correlation structure should contain some displaced eigenvalues, that is, at least some of the eigenvalues are outside the RMT bounds of (3). The validity of this hypothesis will be discussed in Section III.

D. DATA ANALYSES

Data analyses were performed to assess the differences between individuals belonging to two age groups by using the tested features. To compare the proposed approach with the conventional method, in addition to the correlation matrix eigenvalues, the tested features also included a COP velocity feature. The COP velocity is typically characterized by its mean velocity (MV), its MV in the ML direction (MV_{ML}), and its MV in the AP direction (MV_{AP}). This study chose MV_{AP} as the benchmark COP feature because it has been considered the most sensitive measure in the assessment of postural balance performance [5], [43], [44] and is considered one of the best traditional COP features in identifying older people with high fall risk [20]. For the sake of comparison, this study also reports the results obtained by MV_{ML} .

Considering the possible nonstationarity of the FP-GRF signals and by assuming these signals to be stationary for a short duration, we used a sliding window method to determine the correlation matrices. As shown in Fig. 2, a sliding window of width T is moved along the signals with a step size ΔT . The correlation coefficients of all signal pairs can be computed for each of these sliding windows. For the k -th window, such a correlation coefficient between the i -th and j -th signals is denoted as $c_{ij}[k]$. With c_{ij} representing the i -th row and j -th column element of the correlation matrix $C[k]$, the corresponding eigenvalues and eigenvectors can then be determined by solving the eigenvalue problem. After sorting the eigenvalues in ascending order, the vector of the eigenvalues is defined as $\lambda = [\lambda_1, \lambda_2, \dots, \lambda_8]^T$. In this work, the length of the sliding window T was chosen as 1 s. The step size ΔT of the sliding window was chosen as 0.125 s. Therefore, for a signal length of 30 s, the number of windows was 233 (29 s/0.125 s + 1).

To demonstrate the effectiveness of the proposed approach, we first used a standard statistical test procedure to compare the two age groups. We denoted the i -th eigenvalue population means of the younger and older populations as $\bar{\lambda}_i^{YP}$ and $\bar{\lambda}_i^{OP}$, respectively, and performed two-sided t-tests to determine

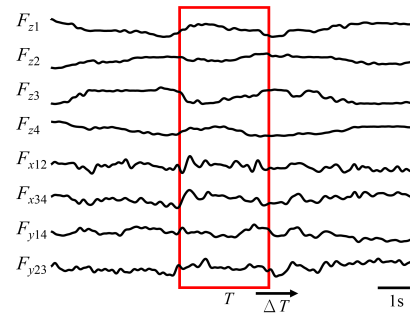


FIGURE 2. Sliding window method employed in this work to determine the correlation matrix of the signals of GRF components.

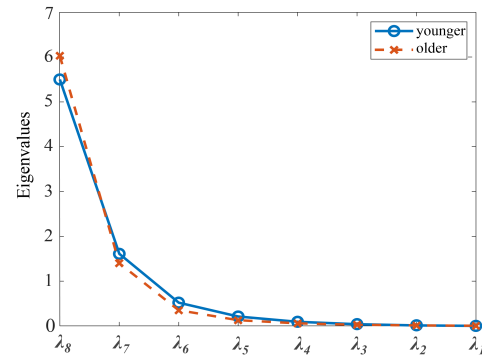


FIGURE 3. Eigenvalues of the younger and older age groups.

whether the value of $\bar{\lambda}_i^{YP}$ was different from the value of $\bar{\lambda}_i^{OP}$. The difference was considered significant if the p -value was < 0.05 .

To set up the samples for the statistical tests, for a given test participant, the value of the i -th eigenvalue associated with the k -th window of the j -th experimental trial was denoted as $\lambda_i(j, k)$ for $j = 1, \dots, 12$ (12 trials/person), and $k = 1, \dots, 233$ (233 windows/trial). By averaging this variable over the sliding windows and the experimental trials, the sample value of the i -th eigenvalue was determined using

$$\lambda_i = \frac{1}{2796} \sum_{j=1}^{12} \sum_{k=1}^{233} \lambda_i(j, k) \quad (11)$$

The statistical test results are summarized in Table 1. Table 1 also presents the results of the benchmark COP feature. To illustrate the distribution patterns of the eigenvalues, the sample means of the eigenvalues are plotted in Fig. 3 for both age groups.

To further compare the effectiveness of the proposed features, we used a binary classification method to classify the younger and older age groups by using the tested features. To use a larger data set to verify the effectiveness of the proposed approach, we employed a simple data augmentation technique to increase the size of the dataset. As mentioned earlier, we conducted 12 trials (4 sessions \times 3 trials/session) with each test participant, and therefore, the number of possible combinations for selecting three objects from 12 objects

TABLE 1. Statistical Test Results of Tested Features Obtained from 3D GRF Components.

Features	Groups		p-values
	Younger group	Older group	
MV_{AP}	5.45±0.97	7.28±1.99	6.82×10^{-4}
MV_{ML}	4.47±1.05	4.23±0.83	0.443
λ_8	5.50±0.248	6.03±0.245	5.02×10^{-8}
λ_7	1.61±0.165	1.40±0.174	3.95×10^{-4}
λ_6	$0.522 \pm 7.15 \times 10^{-2}$	$0.350 \pm 5.69 \times 10^{-2}$	3.08×10^{-10}
λ_5	$0.213 \pm 4.52 \times 10^{-2}$	$0.127 \pm 3.33 \times 10^{-2}$	3.91×10^{-8}
λ_4	$9.54 \times 10^{-2} \pm 2.44 \times 10^{-2}$	$5.64 \times 10^{-2} \pm 1.75 \times 10^{-2}$	1.06×10^{-6}
λ_3	$4.09 \times 10^{-2} \pm 1.15 \times 10^{-2}$	$2.51 \times 10^{-2} \pm 8.66 \times 10^{-3}$	1.79×10^{-5}
λ_2	$1.52 \times 10^{-2} \pm 4.75 \times 10^{-3}$	$1.00 \times 10^{-2} \pm 3.78 \times 10^{-3}$	4.64×10^{-4}
λ_1	$4.19 \times 10^{-3} \pm 1.46 \times 10^{-3}$	$2.92 \times 10^{-3} \pm 1.22 \times 10^{-3}$	5.05×10^{-3}

Values in the second and third columns are mean ± standard deviation. Units of features: Dimensionless λ_i ; mm/s (MV_{AP}).

is 220. By using the average of three trial results as the test sample, we could generate 220 samples for each participant by using the data augmentation technique. Consequently, the number of samples of each age group increased from 240 (12 measures/person × 20 persons) to 4400 (220 measures/person × 20 persons).

When performing the classification tests, each of the tested features was independently used to classify the two age groups. When solving these binary classification problems, we assumed that the mean of the tested feature of the positive class was larger than that of the negative class.

When classifying any given sample data point, if its feature value was larger than a specified threshold, the classifier assigned this data point to the positive class. Otherwise, this data point was assigned to the negative class. If a positive class sample data point was correctly classified as positive, it was counted as a true positive, and if a negative class sample data point was classified as positive, it was counted as a false positive. The true and false positive rates vary with the value of the threshold. By sweeping the threshold from the lowest to the highest sample data values, a receiver operating characteristic (ROC) curve was generated by plotting the true positive rate as a function of the false positive rate. The area under the curve (AUC) of the ROC curve was computed and reported in this work. The AUC represents an estimate of the probability that a classifier ranks a randomly chosen positive example higher than a randomly chosen negative example [45].

Accuracy was defined as the proportion of correctly classified samples; in this study, we chose the optimal operating point of the ROC curve as the point that yields the highest classification accuracy. Sensitivity was defined as the proportion of correctly classified older age group samples, and specificity as the proportion of correctly classified younger group samples. This study used accuracy, sensitivity, and specificity associated with the optimal operating point of the ROC curve to characterize the classification results. The classification test results are summarized in Table 2.

The basic version of the proposed approach assumes that the force plate can measure three-dimensional (3D) GRF components. However, this approach can be directly

TABLE 2. Classification Results of Tested Features Obtained from 3D GRF Components.

Features	Classification Results			
	AUC	Accuracy	Sensitivity	Specificity
MV_{AP}	0.778	0.733	0.915	0.550
MV_{ML}	0.545	0.545	0.353	0.738
λ_8	0.923	0.858	0.755	0.961
λ_7	0.782	0.714	0.549	0.878
λ_6	0.971	0.904	0.887	0.921
λ_5	0.928	0.854	0.828	0.881
λ_4	0.893	0.809	0.731	0.887
λ_2	0.854	0.778	0.735	0.821
λ_2	0.794	0.739	0.776	0.703
λ_1	0.740	0.701	0.734	0.668

adapted to force plates that can only measure the GRF components in the vertical direction: F_{1z} , F_{2z} , F_{3z} , and F_{4z} . The following reasons can justify such a simplification. First, one-dimensional (1D) force sensors are much more affordable than 3D force sensors. Therefore, the cost of the measurement system can be considerably reduced. Second, because of the gravitational force in the vertical direction, the GRF components in the vertical direction are considerably larger than the GRF components in the horizontal direction during quiet standing. Therefore, the GRF components in the AP and ML directions are often considered negligible when computing the COP during quiet standing [46], [47]. This is also the reason that the Nintendo Wii balance board (Nintendo) is considered a suitable and reliable tool for assessing the performance of standing balance, even though it cannot be used for measuring the horizontal components of the GRF [48]–[50]. The 1D GRF statistical and classification test results obtained by considering only the GRF components in the vertical direction are summarized in Tables 3 and 4, respectively.

Finally, to further test the proposed approach, the tested features were used to differentiate younger age group test subjects in eyes-open and eyes-closed conditions. This is important since it is well known that withdrawal of visual information can degrade postural stability. Similar to Table 2,

TABLE 3. Statistical Test Results of Tested Features Obtained from 1D GRF Components.

Features	Groups		<i>p</i> -values
	Younger group	Older group	
MV_{AP}	5.53±0.99	7.40±2.03	6.82×10^{-4}
MV_{ML}	4.50±1.07	4.27±0.84	0.055
λ_4	3.22±0.136	3.46±0.107	3.26×10^{-7}
λ_3	0.604±0.113	0.434±0.082	3.44×10^{-6}
λ_2	$0.138 \pm 3.77 \times 10^{-2}$	$0.081 \pm 2.72 \times 10^{-2}$	3.03×10^{-6}
λ_1	$0.038 \pm 1.13 \times 10^{-2}$	$0.025 \pm 8.96 \times 10^{-3}$	4.20×10^{-4}

Values in the second and third columns are mean ± standard deviation. Units of features: Dimensionless λ_i ; mm/s (MV_{AP})

TABLE 4. Classification Results of Tested Features Obtained from 1D GRF Components.

Features	Classification Results			
	AUC	Accuracy	Sensitivity	Specificity
MV_{AP}	0.762	0.706	0.821	0.592
MV_{ML}	0.537	0.546	0.521	0.571
λ_4	0.894	0.822	0.734	0.910
λ_3	0.863	0.792	0.690	0.894
λ_2	0.861	0.786	0.690	0.883
λ_1	0.787	0.726	0.728	0.723

the classification results are summarized in Table 5. In this test, sensitivity was defined as the proportion of correctly classified eyes-open samples, and specificity as the proportion of correctly classified eyes-closed group samples.

III. RESULTS AND DISCUSSION

In agreement with previous studies, the benchmark COP feature, that is, the mean MV_{AP} of the older group is significantly higher than that of the younger group (Table 1). Significant statistical test results were achieved for all the eigenvalue features. The mean of the highest eigenvalue (i.e., λ_8) of the older group is significantly higher than that of the younger group. This result indicates that the dominant role of the highest eigenvalue of the older group is more prominent than that of the younger group. By contrast, the means of the remaining eigenvalues of the older group are all significantly lower than those of the younger group.

According to RMT, a condition for eigenvalues to be bounded by (3) is that signals need to be independent of one another. Eigenvalues that show large deviations from the RMT bounds correspond to a genuine multivariate time series correlation structure. As discussed in Section II.C, with three balance task constraints, the FP-GRF signals cannot be all mutually independent. Therefore, we hypothesized that some of the eigenvalues should be outside the RMT bounds of (3).

With $L = 512$ (1 s window with a 512-Hz sampling rate) and $N = 8$ (eight channels of FP-GRF signals), the eigenvalue bounds associated with (3) are [0.765 1.265]. As shown in Table 1, the eigenvalues obtained in this work are all outside the RMT bounds. This implies that none of the correlations between the FP-GRF signals are random. However,

TABLE 5. Classification Results of Tested Features Obtained from 3D GRF Components for assessing the visual effects of the younger age group.

Features	Classification Results			
	AUC	Accuracy	Sensitivity	Specificity
MV_{AP}	0.687	0.621	0.855	0.387
MV_{ML}	0.563	0.553	0.545	0.561
λ_8	0.718	0.664	0.572	0.757
λ_7	0.716	0.660	0.564	0.756
λ_6	0.667	0.603	0.887	0.318
λ_5	0.634	0.602	0.747	0.457
λ_4	0.602	0.578	0.550	0.606
λ_3	0.599	0.571	0.437	0.705
λ_2	0.585	0.558	0.380	0.735
λ_1	0.562	0.547	0.528	0.566

this finding is not conclusive because the requirements of $L \rightarrow \infty$ and $N \rightarrow \infty$ have not been met. Nevertheless, several other observations also support the existence of non-random correlations in the GRF correlation structure.

The first observation, as inferred from Fig. 3, is that there is a clear separation of the highest eigenvalue from the remaining eigenvalues in both age groups. The implications of such an eigenvalue distribution pattern can be illustrated by considering two extreme correlation structure cases. In the first case, all signals are assumed to perfectly correlate with one another. By recalling that the sum of the eigenvalues is N , this spectrum of eigenvalues has only one nonzero eigenvalue, $\lambda_N = N$, and thus exhibits a centralized distribution pattern. In the second extreme case, all signals are all mutually independent and thus uncorrelated. In this case, we have a uniform eigenvalue distribution pattern of $\lambda_i = 1$ for $i = 1, \dots, N$. The results shown in Fig. 3 are very different from the uniform distribution pattern and resemble the centralized distribution behavior. Thus, Fig. 3 supports the existence of nonrandom correlations in the GRF correlation structure. In fact, a previous work found that a repulsion between the highest eigenvalue and the remaining eigenvalues occurs when all signals are simultaneously correlated [38].

The second observation is related to the probability distribution function predicted by RMT. If the correlations between the FP-GRF signals are all random, the probability distribution function of the eigenvalues should be represented by (2). If this is indeed the case, the eigenvalues of the younger and older age groups should have the same probability distribution function and their eigenvalues should therefore be identical. However, as seen in Table 1, the means of eigenvalues of the two age groups are all significantly different. In addition, the results in Table 2 indicate that the differences between the eigenvalues can effectively help distinguish between the two age groups. Therefore, these results appear to suggest that the two age groups have different nonrandom correlation properties, which can help differentiate between individuals of the two age groups.

In addition to the identification of the nonrandom correlations of the GRF correlation structure, the issue that warrants investigation is the impact of the horizontal GRF components. As mentioned in Section II.D, when computing the COP by using (8) and (9), the contributions of the horizontal GRF components were considered negligible for quiet standing. This assumption is supported by our results. As seen in Tables 1 and 3, the MV_{AP} values obtained from 3D and 1D GRF signals are similar. Furthermore, by only considering the vertical GRF components, we observe that the statistical and classification test results presented in Tables 3 and 4 are in accordance with the results presented in Tables 1 and 2, respectively. A comparison between the 1D GRF correlation structures of the two age groups shows that the means of the correlation matrix eigenvalues are all significantly different (Table 3) suggesting that these eigenvalues can still be used to effectively differentiate between individuals belonging to the two age groups (Table 4). However, the results of Table 4 are inferior to the results of Table 2. In specific, the highest AUC and accuracy in Table 2 are 0.971 and 0.904 (obtained by λ_6), respectively. In comparison, the highest AUC and accuracy in Table 4 are 0.894 and 0.822 (obtained by λ_4), respectively. Such differences suggest that the horizontal GRF components play an important role in characterizing the GRF correlation structure and should be considered when assessing postural stability.

Finally, Table 5 summarizes the classification results of the tested features for differentiating the eyes-open and eyes-closed experimental data of the younger age group. Results of Table 2 and Table 5 demonstrate that the tested features are less effective in assessing the impact on postural stability caused by visual effect than that caused by the aging effect. However, in differentiating the visual effect on the younger age group, two of the proposed features (λ_7 and λ_8), are still able to provide better results than the benchmark COP feature MV_{AP} .

To further investigate the potential of the proposed approach in assessing postural stability, we should adapt the proposed approach to allow it to be used with different GRF measurement devices in future work. For example, by placing pressure sensors under different areas of the foot, many instrumented insoles can measure multiple GRF components [51]–[55]. By studying the GRF correlation structure associated with these instrumented insoles, the proposed approach can be used to study human walking and running behaviors.

IV. CONCLUSION

As the only variable force applied to the human body during quiet standing, the GRF plays a crucial role in postural balance. When measured using force plates, the GRF is decomposed into multiple components. Therefore, when standing on a force plate, our postural control system needs to coordinate these force components to maintain stable posture. Despite the postural stability being closely related to these GRF components, the interactions between postural stability and GRF components have rarely been studied.

Based on RMT, we proposed a systematic approach to analyze the correlation structure of these GRF signals. We determined their correlation matrix and then solved the corresponding eigenvalue problems; we then used the resulting eigenvalues to characterize postural stability. The effectiveness of the proposed features was demonstrated by comparing the GRF correlation structures of individuals belonging to two age groups via experiments in which the individuals were in the quiet standing posture.

The experimental results reveal the following. First, our results agree with the analytical results obtained using RMT, which predict the eigenvalue bounds for mutually independent signals. Because the GRF components are constrained for several balance tasks and therefore cannot be all mutually independent, some of the eigenvalues should be outside the RMT bounds. This hypothesis was at least partially supported by our experimental results because the eigenvalues obtained in this study were all outside the RMT bounds. Second, statistical and classification test results demonstrated that the eigenvalues of the GRF correlation structure can effectively differentiate between the two age groups. Therefore, we conclude that the GRF correlation structure is age dependent. The third finding relates to the horizontal GRF components, which have been considered negligible during quiet standing. However, by comparing the classification test results obtained from 1D and 3D GRF components, we found that the horizontal GRF components provide valuable information for postural stability assessment and therefore should not be completely ignored.

Considering the simplicity and effectiveness of the proposed features, a possible future work is to extensively test the effectiveness of the proposed features in characterizing the impact of many health-related conditions that could impair postural stability. Another possible future work is to adapt the proposed approach to other GRF measurement devices such as instrumented insoles.

ACKNOWLEDGMENT

This research was partly supported by the Ministry of Science and Technology in Taiwan (R. O. C.), under grants 106-2221-E-110-044 and MOST 107-2221-E-110-073.

COMPETING INTERESTS

The authors declare that they have no competing interests.

REFERENCES

- [1] D. Winter, "Human balance and posture control during standing and walking," *Gait Posture*, vol. 3, no. 4, pp. 193–214, Dec. 1995.
- [2] D. A. Winter, A. E. Patla, F. Prince, M. Ishac, and K. Giello-Periczak, "Stiffness control of balance in quiet standing," *J. Neurophysiol.*, vol. 80, no. 3, pp. 1211–1221, Sep. 1998.
- [3] A. Crétual, "Which biomechanical models are currently used in standing posture analysis?" *Neurophysiol. Clinique*, vol. 45, nos. 4–5, pp. 285–295, Nov. 2015.
- [4] T. Paillard and F. Noé, "Techniques and methods for testing the postural function in healthy and pathological subjects," *BioMed Res. Int.*, vol. 2015, Oct. 2015, Art. no. 891390.
- [5] T. E. Prieto, J. B. Myklebust, R. G. Hoffmann, E. G. Lovett, and B. M. Myklebust, "Measures of postural steadiness: Differences between healthy young and elderly adults," *IEEE Trans. Biomed. Eng.*, vol. 43, no. 9, pp. 956–966, Sep. 1996.

- [6] M. Duarte and D. Sternad, "Complexity of human postural control in young and older adults during prolonged standing," *Exp. Brain Res.*, vol. 191, no. 3, pp. 265–276, Nov. 2008.
- [7] S. Fioretti, M. Scocco, L. Ladislao, G. Ghetti, and R. A. Rabini, "Identification of peripheral neuropathy in type-2 diabetic subjects by static posturography and linear discriminant analysis," *Gait Posture*, vol. 32, no. 3, pp. 317–320, Jul. 2010.
- [8] M. Mazaheri, H. Negahban, M. Salavati, M. A. Sanjari, and M. Parnianpour, "Reliability of recurrence quantification analysis measures of the center of pressure during standing in individuals with musculoskeletal disorders," *Med. Eng. Phys.*, vol. 32, no. 7, pp. 808–812, Sep. 2010.
- [9] A. Mansfield, C. J. Danells, J. L. Zettel, S. E. Black, and W. E. McIlroy, "Determinants and consequences for standing balance of spontaneous weight-bearing on the paretic side among individuals with chronic stroke," *Gait Posture*, vol. 38, no. 3, pp. 428–432, Jul. 2013.
- [10] D. Gasq, M. Labrunée, D. Amarantini, P. Dupui, R. Montoya, and P. Marque, "Between-day reliability of centre of pressure measures for balance assessment in hemiplegic stroke patients," *J. Neuroeng. Rehabil.*, vol. 11, no. 1, p. 39, 2014.
- [11] F. Tamburella, G. Scivoletto, M. Iosa, and M. Molinari, "Reliability, validity, and effectiveness of center of pressure parameters in assessing stabilometric platform in subjects with incomplete spinal cord injury: A serial cross-sectional study," *J. Neuroeng. Rehabil.*, vol. 11, no. 1, p. 86, 2014.
- [12] P. C. Fino, M. A. Nussbaum, and P. G. Brolinson, "Decreased high-frequency center-of-pressure complexity in recently concussed asymptomatic athletes," *Gait Posture*, vol. 50, pp. 69–74, Oct. 2016.
- [13] A. C. Schmitt, C. P. Repka, G. D. Heise, J. H. Challis, and J. D. Smith, "Comparison of posture and balance in cancer survivors and age-matched controls," *Clin. Biomech.*, vol. 50, pp. 1–6, Dec. 2017.
- [14] V. D. Vassimon-Barroso, A. M. Catai, M. S. D. S. Buto, A. Porta, and A. C. D. M. Takahashi, "Linear and nonlinear analysis of postural control in frailty syndrome," *Brazilian J. Phys. Therapy*, vol. 21, no. 3, pp. 184–191, May 2017.
- [15] Y.-C. Lin, C.-C. Niu, M. Nikkhoo, M.-L. Lu, W.-C. Chen, C.-J. Fu, and C.-H. Cheng, "Postural stability and trunk muscle responses to the static and perturbed balance tasks in individuals with and without symptomatic degenerative lumbar disease," *Gait Posture*, vol. 64, pp. 159–164, Jul. 2018.
- [16] D. A. Jehu, H. Cantù, A. Hill, C. Paquette, J. N. Côté, and J. Nantel, "Medication and trial duration influence postural and pointing parameters during a standing repetitive pointing task in individuals with Parkinson's disease," *PLoS ONE*, vol. 13, no. 4, Apr. 2018, Art. no. e0195322.
- [17] Y. Ninkaido, T. Akisue, Y. Kajimoto, A. Tucker, Y. Kawami, H. Urakami, Y. Iwai, H. Sato, T. Nishiguchi, T. Hinochita, K. Kuroda, H. Ohno, and R. Saura, "Postural instability differences between idiopathic normal pressure hydrocephalus and Parkinson's disease," *Clin. Neurol. Neurosurg.*, vol. 165, pp. 103–107, Feb. 2018.
- [18] D. A. Wajda, R. W. Motl, and J. J. Sosnoff, "Three-month test-retest reliability of center of pressure motion during standing balance in individuals with multiple sclerosis," *Int. J. MS Care*, vol. 18, no. 2, pp. 59–62, Mar. 2016.
- [19] F. Yang and X. Liu, "Relative importance of vision and proprioception in maintaining standing balance in people with multiple sclerosis," *Multiple Sclerosis Rel. Disorders*, vol. 39, Apr. 2020, Art. no. 101901.
- [20] F. Quijoux, A. Vienne-Jumeau, F. Bertin-Hugault, P. Zawieja, M. Lefevre, P.-P. Vidal, and D. Ricard, "Center of pressure displacement characteristics differentiate fall risk in older people: A systematic review with meta-analysis," *Ageing Res. Rev.*, vol. 62, Jun. 2020, Art. no. 101117.
- [21] C.-Y. Hong, L.-Y. Guo, R. Song, M. L. Nagurka, J.-L. Sung, and C.-W. Yen, "Assessing postural stability via the correlation patterns of vertical ground reaction force components," *Biomed. Eng. OnLine*, vol. 15, no. 1, p. 90, Dec. 2016.
- [22] F. J. Dyson, "Statistical theory of the energy levels of complex systems. I, II, III," *J. Math. Phys.*, vol. 3, pp. 140–175, Jan./Feb. 1962.
- [23] F. J. Dyson and M. L. Mehta, "Statistical theory of the energy levels of complex systems. IV," *J. Math. Phys.*, vol. 4, no. 5, pp. 701–712, May 1963.
- [24] M. L. Mehta and F. J. Dyson, "Statistical theory of the energy levels of complex systems. V," *J. Math. Phys.*, vol. 4, no. 5, pp. 713–719, May 1963.
- [25] E. P. Wigner, "On a class of analytic functions from the quantum theory of collisions," *Ann. Math.*, vol. 53, no. 1, pp. 36–67, 1951.
- [26] E. P. Wigner, "On the statistical distribution of the widths and spacings of nuclear resonance levels," *Math. Proc. Cambridge Phil. Soc.*, vol. 47, no. 4, pp. 790–798, Oct. 1951.
- [27] V. Plerou, P. Gopikrishnan, B. Rosenow, L. A. N. Amaral, T. Guhr, and H. E. Stanley, "Random matrix approach to cross correlations in financial data," *Phys. Rev. E, Stat. Phys. Plasmas Fluids Relat. Interdiscip. Top.*, vol. 65, no. 6, Jun. 2002, Art. no. 066126.
- [28] T. Colon, H. Ruskin, and M. Crane, "Random matrix theory and fund of funds portfolio optimization," *Phys. A, Stat. Mech. Appl.*, vol. 382, pp. 565–576, Aug. 2007.
- [29] J. Kwapien, S. Drożdż, and A. Ioannides, "Temporal correlations versus noise in the correlation matrix formalism: An example of the brain auditory response," *Phys. Rev. E, Stat. Phys. Plasmas Fluids Relat. Interdiscip. Top.*, vol. 62, no. 4, p. 5557, 2000.
- [30] M. S. Santhanam and P. K. Patra, "Statistics of atmospheric correlations," *Phys. Rev. E, Stat. Phys. Plasmas Fluids Relat. Interdiscip. Top.*, vol. 64, no. 1, Jun. 2001, Art. no. 016102.
- [31] M. Barthélemy, B. Gondran, and E. Guichard, "Large scale cross-correlations in Internet traffic," *Phys. Rev. E, Stat. Phys. Plasmas Fluids Relat. Interdiscip. Top.*, vol. 66, no. 5, Nov. 2002, Art. no. 056110.
- [32] G. Baier, M. Müller, U. Stephani, and H. Muhle, "Characterizing correlation changes of complex pattern transitions: The case of epileptic activity," *Phys. Lett. A*, vol. 363, no. 4, pp. 290–296, Apr. 2007.
- [33] K. Schindler, H. Leung, C. E. Elger, and K. Lehnertz, "Assessing seizure dynamics by analysing the correlation structure of multichannel intracranial EEG," *Brain*, vol. 130, no. 1, pp. 65–77, Nov. 2006.
- [34] C. Rummel, G. Baier, and M. Müller, "The influence of static correlations on multivariate correlation analysis of the EEG," *J. Neurosci. Methods*, vol. 166, no. 1, pp. 138–157, Oct. 2007.
- [35] H. Gast, K. Schindler, C. Rummel, U. S. Herrmann, C. Roth, C. W. Hess, and J. Mathis, "EEG correlation and power during maintenance of wakefulness test after sleep-deprivation," *Clin. Neurophysiol.*, vol. 122, no. 10, pp. 2025–2031, Oct. 2011.
- [36] A. M. Sengupta and P. P. Mitra, "Distributions of singular values for some random matrices," *Phys. Rev. E, Stat. Phys. Plasmas Fluids Relat. Interdiscip. Top.*, vol. 60, no. 3, pp. 3389–3392, Sep. 1999.
- [37] I. T. Jolliffe, "Springer series in statistics," in *Principal Component Analysis*, 2nd ed. New York, NY, USA: Springer-Verlag, 2002.
- [38] M. Müller, G. Baier, A. Galka, U. Stephani, and H. Muhle, "Detection and characterization of changes of the correlation structure in multivariate time series," *Phys. Rev. E, Stat. Phys. Plasmas Fluids Relat. Interdiscip. Top.*, vol. 71, no. 4, Apr. 2005, Art. no. 046116.
- [39] M. Müller, Y. L. Jiménez, C. Rummel, G. Baier, A. Galka, U. Stephani, and H. Muhle, "Localized short-range correlations in the spectrum of the equal-time correlation matrix," *Phys. Rev. E, Stat. Phys. Plasmas Fluids Relat. Interdiscip. Top.*, vol. 74, no. 4, Oct. 2006, Art. no. 041119.
- [40] A. L. Hof, "The equations of motion for a standing human reveal three mechanisms for balance," *J. Biomech.*, vol. 40, no. 2, pp. 451–457, Jan. 2007.
- [41] M. Beaulieu, P. Allard, M. Simoneau, G. Dalleau, F. A. Hazime, and C.-H. Rivard, "Relationship between oscillations about the vertical axis and center of pressure displacements in single and double leg upright stance," *Amer. J. Phys. Med. Rehabil.*, vol. 89, no. 10, pp. 809–816, Oct. 2010.
- [42] D. C. Hay and M. P. Wachowiak, "Analysis of free moment and center of pressure frequency components during quiet standing using magnitude squared coherence," *Hum. Movement Sci.*, vol. 54, pp. 101–109, Aug. 2017.
- [43] V. Cornilleau-Péres, N. Shabana, J. Droulez, J. C. H. Goh, G. S. M. Lee, and P. T. K. Chew, "Measurement of the visual contribution to postural steadiness from the COP movement: Methodology and reliability," *Gait Posture*, vol. 22, no. 2, pp. 96–106, Oct. 2005.
- [44] M. Kouzaki and K. Masani, "Postural sway during quiet standing is related to physiological tremor and muscle volume in young and elderly adults," *Gait Posture*, vol. 35, no. 1, pp. 11–17, Jan. 2012.
- [45] T. Fawcett, "An introduction to ROC analysis," *Pattern Recognit. Lett.*, vol. 27, no. 8, pp. 861–874, Jun. 2006.
- [46] L. Baratto, P. G. Morasso, C. Re, and G. Spada, "A new look at posturographic analysis in the clinical context: Sway-density versus other parameterization techniques," *Motor Control*, vol. 6, no. 3, pp. 246–270, Jul. 2002.
- [47] M. Duarte and S. M. S. F. Freitas, "Revision of posturography based on force plate for balance evaluation," *Rev. Brasileira Fisioterapia*, vol. 14, no. 3, pp. 183–192, 2010.

- [48] D.-S. Park and G. Lee, "Validity and reliability of balance assessment software using the Nintendo Wii balance board: Usability and validation," *J. Neuroeng. Rehabil.*, vol. 11, no. 1, p. 99, 2014.
- [49] J. Lee, G. Webb, A. P. Shortland, R. Edwards, C. Wilce, and G. D. Jones, "Reliability and feasibility of gait initiation centre-of-pressure excursions using a Wii balance board in older adults at risk of falling," *Aging Clin. Exp. Res.*, vol. 31, no. 2, pp. 257–263, Feb. 2019.
- [50] S. Madhavan and S. Pradhan, "Relationship between Nintendo's Wii balance board derived variables and clinical balance scores in individuals with stroke," *Gait Posture*, vol. 79, pp. 170–174, Jun. 2020.
- [51] D. A. Jacobs and D. P. Ferris, "Estimation of ground reaction forces and ankle moment with multiple, low-cost sensors," *J. Neuroeng. Rehabil.*, vol. 12, no. 1, p. 90, Oct. 2015.
- [52] X. Hu, J. Zhao, D. Peng, Z. Sun, and X. Qu, "Estimation of foot plantar center of pressure trajectories with low-cost instrumented insoles using an individual-specific nonlinear model," *Sensors*, vol. 18, no. 2, p. 421, Feb. 2018.
- [53] R. Eguchi, A. Yoroze, T. Fukumoto, and M. Takahashi, "Estimation of vertical ground reaction force using low-cost insole with force plate-free learning from single leg stance and walking," *IEEE J. Biomed. Health Inform.*, vol. 24, pp. 1276–1283, May 2020.
- [54] A. Ngueleu, A. Blanchette, L. Bouyer, D. Maltais, B. McFadyen, H. Moffet, and C. Batcho, "Design and accuracy of an instrumented insole using pressure sensors for step count," *Sensors*, vol. 19, no. 5, p. 984, Feb. 2019.
- [55] A. M. Tahir, M. E. H. Chowdhury, A. Khandakar, S. Al-Hamouz, M. Abdalla, S. Awadallah, M. B. I. Reaz, and N. Al-Emadi, "A systematic approach to the design and characterization of a smart insole for detecting vertical ground reaction force (vGRF) in gait analysis," *Sensors*, vol. 20, no. 4, p. 957, Feb. 2020.



JIA-LI SUNG was born in Hualien, Taiwan, in 1988. He received the B.S. degree in industrial education and technology and the M.S. degree in mechatronics engineering from the National Changhua University of Education, Changhua, Taiwan, in 2011 and 2014, respectively. He is currently pursuing the Ph.D. degree in mechanical and electro-mechanical engineering with National Sun Yat-sen University, Kaohsiung, Taiwan. He was an Intern with Takumi Machinery Company Ltd., Taichung, Taiwan, in 2012. From 2017 to 2020, he was an Assistant Engineer with Soteria Biotech Company Ltd., New Taipei City, Taiwan. His research interests include the digital/physiological signal processing, EEG time-frequency analysis, and machine/deep learning.



LAN-YUEN GUO received the B.S. degree in physical therapy from National Yang-Ming University, Taipei, Taiwan, in 1992, and the M.S. and Ph.D. degrees in biomedical engineering from National Cheng-Kung University, Tainan, Taiwan, in 1996 and 2003, respectively. He had been an Assistant Professor and an Associate Professor with the Department of Sports Medicine, from 2004 to 2012. He has been a Professor with the Department of Sports Medicine, Kaohsiung Medical University, Kaohsiung, Taiwan, since 2012. His research interests include sports medicine, biomechanics, movement science, physical therapy, and rehabilitation engineering.



CHIN-HSUAN LIU received the B.S. degree in rehabilitation from Kaohsiung Medical University, Kaohsiung, Taiwan, in 2001, the M.Ed. degree from National Kaohsiung Normal University, Kaohsiung, and the Ph.D. degree in computer science and information engineering from the National Taipei University of Technology, Taipei, Taiwan. She has been an Occupational Therapist with the Kaohsiung Municipal Kai-Syuan Psychiatric Hospital and a Lecturer with I-Shou University. Her research interests include mental illness, motion analysis, rehabilitation, and artificial intelligence.



POSEEN LEE received the B.S. degree from Kaohsiung Medical University, Taiwan, the M.A. degree from New York University, USA, and the Ph.D. degree from National Kaohsiung Normal University, Taiwan. Since 2019, he has been an Associate Professor and the Chair with the Department of Occupational Therapy, I-Shou University. His research interests include cognition, schizophrenia, aging, and psychometrics.



CHEN-WEN YEN received the B.E. degree in mechanical engineering from Tamkang University, in 1982, and the M.E. and Ph.D. degrees in mechanical engineering from Carnegie-Mellon University, Pittsburgh, PA, USA, in 1986 and 1989, respectively. Following graduation, he joined the Department of Mechanical Engineering, Sun Yat-sen University, as a Faculty Member. His research interests include machine learning, sleep medicine, intelligent diagnostic systems, and physical therapy and rehabilitation engineering.



LI-HSIUN LIAW received the B.S. degree in physical therapy and the M.S. degree in behavior sciences from Kaohsiung Medical University (KMU), Kaohsiung, Taiwan, in 1993 and 2000, respectively, and the Ph.D. degree in allied health sciences from National Cheng Kung University, Tainan, Taiwan, in 2013.

She has been an Associate Professor with the Department of Physical Therapy, KMU, since 2013. Her research interests include the development of balance and movement training equipment for neurological impaired patients, evaluation of core stability and core strengthening exercises, women's health, and physical therapy. She is also the Vice Chairman of the committee of the continuity of quality of long-term services for elderly in the Taiwan Physical Therapy Association. She received the 2019 Taiwan National Innovation Award in innovative medical device and diagnostic technique.